ARTICLES

Effect of Pressure and Solvent on Raman Spectra of All-*trans*-β-Carotene

Wei-Long Liu,[†] Zhi-Ren Zheng,*[,†] Rui-Bin Zhu,[†] Zhi-Guo Liu,[†] Da-Peng Xu,[‡] Hua-Min Yu,[‡] Wen-Zhi Wu,[†] Ai-Hua Li,[†] Yan-Qiang Yang,[†] and Wen-Hui Su[†,‡]

Center for Condensed Matter Science and Technology, Harbin Institute of Technology, Harbin 150001, China, and Department of Physics, Ji Lin University, Changchun 130023, China

Received: May 25, 2007; In Final Form: August 3, 2007

The ground state Raman spectra of all-*trans*-β-carotene in *n*-hexane and CS_2 solutions are measured by simultaneously changing the solvent environment and molecular structure under high hydrostatic pressure. The diverse pressure dependencies of several representative Raman bands are explained using a competitive mechanism involving bond length changes and vibronic coupling. It is therefore concluded that (a) the in-phase C═C stretching mode plays an essential role in the conversion of energy from S_1 to S_0 states in carotenoids, (b) internal conversion and intramolecular vibrational redistribution can be accelerated by high pressure, and (c) the environmental effect, but not the structural distortion or π-electron delocalization, is responsible for the spectral properties of a given carotenoid species. These findings revealed the potential of high pressure in exploring the nature of the biological functions of carotenoids.

Introduction

Carotenoids and chlorophylls are the most abundant pigments found in nature. As light-harvesting molecules and photoprotective pigments, carotenoids play an important role in photosynthetic systems.[1,2] Much work has therefore been done on the spectroscopic study and ultrafast dynamics of low-lying excited electronic states of carotenoids[3] for the purpose of elucidating the mechanism of internal conversion (IC), intramolecular vibrational redistribution (IVR), and their geometry dependence.[4,5]

IC and IVR originate from the electronic and nuclear vibrations in a molecular system, respectively. Electronic and nuclear degrees of freedom are independent of each other under the Born−Oppenheimer approximation. However, the interaction of these two degrees of freedom, which is called vibronic coupling, must be taken into account in a realistic molecular system. This coupling changes the frequencies of vibrational modes on the one hand and disturbs the energy level of electronic states on the other hand.

Vibronic coupling in polyenes was first proposed to elucidate the unexpected differences between S_0 and S_1 state frequencies of the C═C stretching mode.[6] Orlandi et al. performed detailed quantum mechanical calculations and analyzed the adiabatic vibronic couplings among the lowest electronic states. According to their theory, the adiabatic vibrational frequency of the *k*th mode in the *i*th electronic state can be generally expressed as[7]

$$\omega_{ik} = [\Omega_k^2 + \sum_{i \neq j} 2\Omega_k V_{ij}^{(k)2} (E_i^0 - E_j^0)^{-1}]^{1/2} \quad (1)$$

where Ω_k is the diabatic vibrational frequency of the *k*th mode, $V_{ij}^{(k)}$ is the adiabatic vibronic integral, which describes the coupling of the *i*th and *j*th electronic states by the *k*th normal mode and is discussed in detail by Nagae et al.,[8] and $E_{i(j)}^0$ is the excitation energy of the *i*(*j*)th electronic state. As "diabatic" means that the electron density change with respect to the nuclear displacement is ignored in this theory, Ω_k is independent of electronic states and only dependent on the structure of the molecule. When the vibronic coupling by the *k*th mode is strong between the a state and b state only, the adiabatic frequencies can be expressed as[8]

$$\omega_{a(b)k} \approx \Omega_k \pm \frac{(V_{ab}^k)^2}{\hbar(E_a^0 - E_b^0)} \quad (2)$$

and therefore, the adiabatic frequency of the lower state decreases while that of the upper state increases by the same amount.

The vibronic coupling in β-carotene has been extensively studied using various experimental and theoretical methods. Raman transition was mainly used to attain the coupling information. The first experimental proof of the vibronic coupling in β-carotene was provided by the picosecond transient resonance Raman spectra.[9] The large frequency difference of the C═C stretching mode between the S_0 and S_1 states was explained using the vibronic coupling between these two states. The vibronic coupling was also used to elucidate the effect of solvent on the C═C stretching mode in the S_1 state of β-carotene.[10] The effect of temperature and the isotope on the internal conversion of β-carotene revealed the essential role of

* To whom correspondence should be addressed. E-mail: zrzheng@hit.edu.cn. Phone: +86-451-8641-8583. Fax: +86-451-8641-8440.
[†] Harbin Institute of Technology.
[‡] Ji Lin University.

10.1021/jp074048b CCC: $37.00
Published on Web 09/20/2007

the in-phase C═C stretching mode in the vibronic coupling between the S_1 and S_0 states.[11] Yoshizawa et al. invented the femtosecond Raman spectroscopy technique to research the vibrational relaxation of the S_1 state. The lower frequency of the $1 \rightarrow 2$ transition (as compared with the $0 \rightarrow 1$ transition) in the S_1 state was ascribed to the vibronic coupling between the S_1 and S_0 states.[12] The vibrational relaxation of the S_2 state was also investigated by femtosecond time-resolved stimulated Raman spectroscopy.[13] The observed frequency shifts of the Raman bands in the S_2 state were in agreement with the theoretical predictions considering vibronic coupling. These results exemplified the significance of vibronic coupling in the ultrafast IC and IVR processes of carotenoids.

A general knowledge of the properties of carotenoids in solution is the prerequisite for understanding their functions in more complex natural and artificial systems. The obvious difference between the solvent environment and native living organisms justifies the need for a reasonable conjunction between the photochemical properties of carotenoids in those two matrices. The absorption maxima of a single carotenoid species can be shifted over a wide range by highly specific interactions with proteins.[14] The comparability of this shift with high pressure absorption makes it possible to mimic the effect of the native environment on carotenoids.[15] The continuous tuning of the solution properties over a considerable range can be achieved by applying external hydrostatic pressure. In addition, the application of hydrostatic pressure can also amplify some intramolecular and intermolecular interactions to make them easier to be investigated. The spectral properties of solvated β-carotene have been extensively investigated at normal pressure, but to the best of our knowledge, what has been done in a high pressure study is just a few theoretical models for the effect of pressure on electronic absorption spectra and the resonance Raman excitation profile, not the effect of solvent and pressure on Raman-active modes.[15,16]

Therefore, we measured the ground-state Raman spectra of all-*trans*-β-carotene (referred to hereafter as β-carotene) in *n*-hexane and CS_2 under high pressure and compared the effect of pressure on several representative Raman bands in these two solutions.

Experimental Methods

The β-carotene used was purchased from Sigma-Aldrich, stored at −20 °C in the dark, and used without further purification. The amount of the 15-*cis* isomer was negligible because almost no absorption band was observed around 340 nm before the measurements.[5] In order to enhance the signal, β-carotene was dissolved in CS_2 (analytical grade) or *n*-hexane (HPLC grade) to achieve a saturated solution. In all of the experiments, fresh solution was used immediately after its preparation to avoid degeneration. No crystal was precipitated out during measurements under high pressure.

Quasi-hydrostatic pressure was applied to the sample using a conventional diamond anvil cell (DAC).[17] Two diamonds with 0.5 mm culet faces were used. The gasket was made of stainless steel with an initial thickness of 0.3 mm and had a hole with an initial diameter of 0.25 mm. The pressure inside of the cell was determined by observing the shift of fluorescence (R_1 line) from a small ruby contained within the sample cell.[18]

Both Raman spectra and ruby fluorescence measurements were made with a Raman microscope (Jobin Yvon, HR800) equipped with a neon−helium laser (632.8 nm). The laser power was 20 mW at the sample. For both the normal and high-pressure experiments, the instrumental resolution was 1 cm^{-1}, and therefore, the error of pressure calibration was ± 0.07 GPa. All of the experiments were performed at room temperature in a dark room.

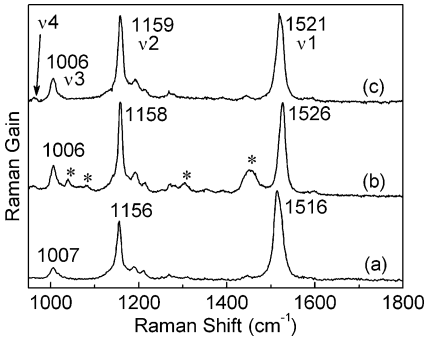

Figure 1. Raman spectra of β-carotene in (a) the solid state, (b) *n*-hexane, and (c) CS_2 at normal pressure. Asterisks in (b) indicate Raman bands from *n*-hexane.

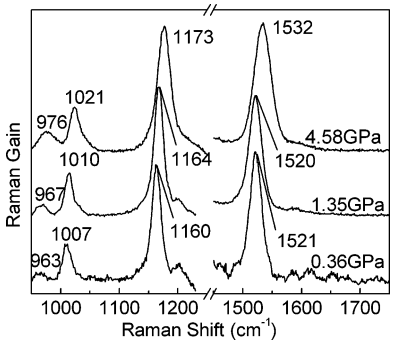

Figure 2. Raman spectra of β-carotene in CS_2 under high pressure. The spectral region from 1250 to 1450 cm^{-1} is cut off because of the intense ruby fluorescence and diamond Raman bands.

Results and Discussion

The Raman spectra of β-carotene in the solid state and in solution at normal pressure are shown in Figure 1. The Raman spectroscopy of crystalline β-carotene is dominated by three main bands, which are located at 1516, 1156, and 1007 cm^{-1} and are called the ν1, ν2, and ν3 bands in Figure 1a. Normal-coordinate analyses have assigned these three bands to C═C in-phase stretching, C−C stretching, and methyl in-plane rocking modes, respectively.[19] The weak band around 960 cm^{-1} in solution is called the ν4 band in Figure 1b and c and is assigned to the C−H out-of-plane wagging.[19]

The solidified pressures measured in our experiment are ∼1.45 and ∼1.35 GPa for *n*-hexane and CS_2 solutions, respectively, which are in good agreement with the literature.[20,21] Several representative Raman spectra in CS_2 are shown in Figure 2. A Lorentzian curve fitting routine was used to determine the center frequency and bandwidth of Raman bands; the changes in the peak positions of the ν1 and ν2 bands were determined with reasonable confidence because of their sharp intensity in both solutions. In order to systematically study the effect of pressure, the changes of the ν1 and ν2 frequencies in *n*-hexane and CS_2 solutions are plotted versus pressure in Figures 3 and 4. The pressure dependences were fitted with liner functions.

Figure 3 shows the pressure dependence of the ν1 and ν2 modes in *n*-hexane before solidification. The slopes of both bands are positive, but ν2 increases more rapidly than the ν1 mode. In the CS_2 solution (as shown in Figure 4), the ν2 band increases at almost the same speed as that in the *n*-hexane solution, while the ν1 band shows an interesting negative slope

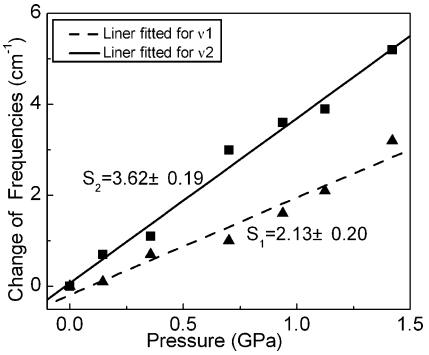

Figure 3. Effect of pressure on Raman frequencies of β-carotene in *n*-hexane. The changes in the Raman frequencies relative to ambient pressure are shown for the $\nu 1$ (▲) and $\nu 2$ (■) bands. The slopes (S) obtained from liner fitting are also presented in the graph with frequency in cm^{-1} and pressure in GPa.

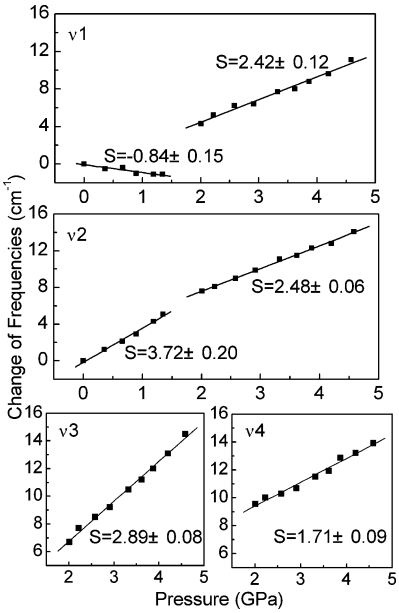

Figure 4. Pressure dependence of the $\nu 1$ and $\nu 2$ frequencies of β-carotene in CS_2. The Raman shifts of the $\nu 3$ and $\nu 4$ bands in a higher pressure range are also presented to illustrate the effect of pressure on Raman modes after the solutions are solidified.

before solidification. Both of the bands move to higher frequencies at the same speed after the solution is solidified.

Moroni et al. have studied the crystalline all-*trans* retinal under pressure.[22] The *trans* → *cis* isomerization in the crystal state under pressure and in the presence of 647.1 nm excitation light was suggested by the Raman spectrum in the fingerprint region. It can be seen by comparing our results with the Raman spectra of *cis*-β-carotene isomers, in which the $\nu 1$ band frequencies of all of the *cis* isomers are higher than that of the all-*trans* isomer,[23] that no *cis* isomer appeared in solution under high pressure during our experiments. A competitive mechanism is therefore proposed to explain our results.

A. Competitive Mechanism under High Pressure. Noguchi et al. have investigated the effect of solvent on the C═C stretching mode in the S_1 state of β-carotene.[10] Although they focused their attention on the larger change in the C═C stretching mode in the S_1 state, there exists the effect of solvent on this mode in the S_0 state. Figure 6 of ref 10 shows a weak, but clearly visible, effect of solvent polarizability on the C═C stretching frequency in the S_0 state. The same effect of solvent can also be found in spheroidene, and it is ascribed to the solvent polarizability dependence of the energy level of S_1[14] As shown

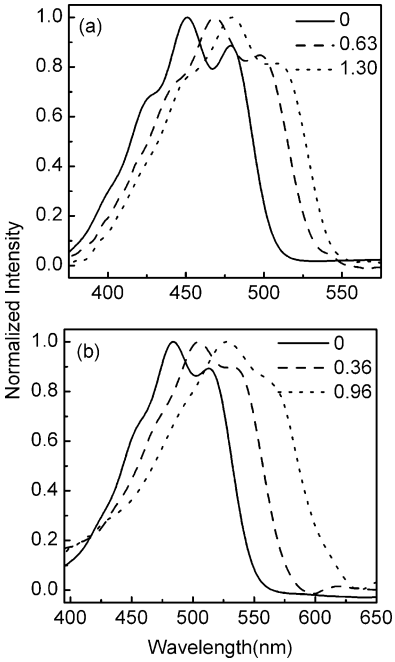

Figure 5. Pressure-dependent absorption spectra of β-carotene in (a) *n*-hexane at 0, 0.63, and 1.3 GPa and (b) CS_2 at 0, 0.36, and 0.96 GPa. The absorption maxima at normal pressure are 451 nm in *n*-hexane and 485 nm in CS_2. Under high pressure, the absorption maximum red shifts by 28 nm to 479 nm in *n*-hexane at 1.30 GPa, while it red shifts by 43 nm to 528 nm in CS_2 at 0.96 GPa. The absorption maximum increases more rapidly in CS_2 than that in *n*-hexane.

in Figure 1, our data can also show the effect of solvent on the $\nu 1$ mode. The lower wavenumber of the $\nu 1$ band (1521 cm^{-1}) in CS_2 compared to that in *n*-hexane (1526 cm^{-1}) is rooted in the lower S_1 energy level. It is generally accepted that the effect of nonpolar solvent on the absorption transition of the nonpolar solute mainly stems from the dispersive interactions, which originate from the induced dipole moment of solute and solvent molecules. Therefore, the interaction between nonpolar carotenoids and nonpolar solvent molecules is mainly dispersive interaction, and it has its effect on both the S_1 and S_2 levels.[24] With the pressure increasing, the following two circumstances appear in the solutions: (a) The increased solvent polarizability induced by high pressure[15] leads to lower energy levels in both solvents; and (b) CS_2 molecules move closer to each other, and parallel configurations between the nearest neighbors are favored under high pressure,[21] but this is not the case in *n*-hexane.[20] The remarkable orientational feature can lead to stronger dispersive interactions, and therefore, there is more sensitive pressure dependence of energy levels in CS_2 than those in *n*-hexane. By comparing the pressure-dependent absorption spectra of β-carotene in these two solvents shown in Figure 5, it can be seen that the S_2 energy level is more sensitive to pressure in CS_2 than in *n*-hexane. As both the S_1 and S_2 energy levels are influenced by the same cause, we can also safely come to the conclusion that the S_1 energy level in CS_2 is more sensitive to pressure than that in *n*-hexane. In addition, the strength of the adiabatic vibronic integral, which is correlated with the transition bond-order matrices and the L matrix,[8] changes when the molecule is exposed to high hydrostatic pressure. The pressure-related adiabatic vibronic integral is also relevant to the Raman-active modes. Accordingly, both the adiabatic vibronic integral and the S_1 energy level can change the adiabatic frequencies under high pressure. The combined contribution of these two factors is called vibronic coupling (VC).[10]

On the basis of the above discussion, a pressure-relevant competitive mechanism is proposed. The adiabatic frequency of the *i*th vibration mode in the S_0 state can be expressed as

$$\omega_i(P) = \Omega_i + \Delta\Omega_i(P) - |V_{01}^{(i)}(P)|^2/E_1(n) \quad (3)$$

where Ω_i is the diabatic frequency of the *i*th vibration mode in the S_0 state at normal pressure, $\Delta\Omega_i(P)$ is the increment of Ω_i as a result of the shortened bond lengths induced by high pressure, and therefore, $\Omega_i + \Delta\Omega_i(P)$ is of diabatic nature and is merely dependent on the equilibrium geometry at a given pressure and is independent of VC. $V_{01}^{(i)}(P)$ is the adiabatic vibronic integral, which describes the coupling of the S_0 and S_1 states through the *ith* normal mode. $E_1(n)$ is the refractive-index-relevant energy level of the S_1 state and is a monotonous decrease function of the solvent refractive index, *n*.[24] Since the solvent refractive index is a monotonous increase function of pressure,[15] the combined contribution of $V_{01}^{(i)}(P)$ and $E_1(n)$ can be expressed as $VC_{01}^{(i)}(P)$. Equation 3 can then be expressed as

$$\omega_i(P) = \Omega_i + \Delta\Omega_i(P) - VC_{01}^{(i)}(P) \quad (4)$$

The VC between the S_0 and S_2 states is not taken into account. All of the following analyses are based on eqs 3 and 4.

(i) Effect of Pressure on the Frequency of the C═C Stretching Mode (i = 1) before Solidification. Although VC is enhanced as $E_1(n)$ decreases in *n*-hexane, $\Delta\Omega_1(P)$ increases at a higher speed so that the total shift of the $\nu1$ band is upward. However, the more sensitive pressure dependence of $E_1(n)$ can exceed the contribution of $\Delta\Omega_1(P)$ in CS_2 and causes a downward shift of the $\nu1$ band.

(ii) Effect of Pressure on the Frequency of the C−C Stretching Mode (i = 2) before Solidification. It can be seen from Figures 3 and 4 that the $\nu2$ band shifts to higher frequencies in both solutions at almost the same speed. According to our competitive mechanism (eq 4), in the two solutions, the $\Delta\Omega_2(P)$ values are equal, while the $E_1(n)$ values are different; thus the adiabatic vibronic integral of the S_0 and S_1 states through the C−C stretching mode must vanish ($V_{01}^{(2)} = 0$, so that $VC_{01}^{(2)}(P) = 0$), and the upward shift of the $\nu2$ frequency is mainly caused by $\Delta\Omega_2(P)$. It is therefore logical to say that the C−C stretching mode does not play any role in S_0 and S_1 coupling, and C═C symmetric stretching modes are the primary acceptor of population from the S_1 state. This is in good agreement with the prevalent viewpoints.[3]

(iii) Effect of Pressure on the Frequency of the Raman Bands in the Solid Phase. As shown above, dispersive interactions are responsible for the interactions between solute and solvent molecules which have their effect on the VC in our experiments. The orientational movement is frozen when the solution is solidified, and the dispersive interactions and the VC then become irrelevant to pressure in our pressure range. The decreased bond length induced by increased pressure is the main cause for the frequency shifts and leads to the same slopes for the $\nu1$ and $\nu2$ modes, as shown in Figure 4. VC exists for the C═C stretching mode, although it is frozen in solid phase, and it is responsible for the changes in the $\nu1$ frequency, which are smaller than those in $\nu2$. Figure 4 also shows the effect of pressure on the $\nu3$ and $\nu4$ modes in the solid phase. The slope of the $\nu3$ ($\nu4$) mode is a little steeper (gentler) than those of the $\nu1$ and $\nu2$ modes. It can be seen from the assignment of the Raman bands of β-carotene[19] that (a) the in-plane rocking of the CH_3 groups is more sensitive to pressure than CC stretching, and (b) the in-plane vibrations show a stronger pressure dependence, while the out-of-plane wagging is less effected by pressure. Therefore, we speculate that the plane of the solidified CS_2 molecules may be vertical to that of β-carotene molecules, which tends to give less effect on the out-of-plane wagging.

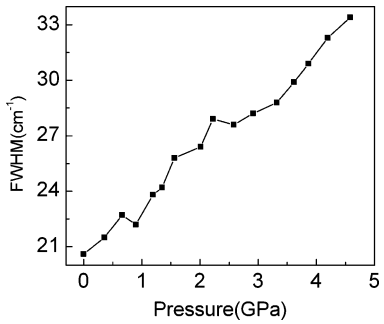

Figure 6. Bandwidth (fwhm) of the $\nu1$ band versus pressure in CS_2.

Another result, which must be mentioned, is that the slope of the $\nu2$ band in the solid phase is not as steep as that in liquid phase. This can be easily understood; the upward shift of the $\nu2$ frequency is mainly ascribed to the shortened bond lengths, and the difficulty in changing the bond lengths leads to a gentle slope of the $\nu2$ band in a solid environment.

(iv) Separation of the Contributions of Bond Length Changes and VC. The same slope (∼2.45) in Figure 4 ($\nu1$ and $\nu2$) after the solution is solidified implies the approximately equal compressibilities of the C═C and C−C bonds. This indicates that the $\Delta\Omega_i(P)$ values are equal for the C═C and C−C modes at a given pressure, namely, $\Delta\Omega_1(P) = \Delta\Omega_2(P)$ in both solutions. This provides the chance to quantitatively separate the contributions of bond length changes and VC.

In order to make a direct comparison, we choose the pressure range of 0−1.3 GPa in both solutions. The slopes of the $\nu2$ bands are 3.62 and 3.72 cm^{-1}/GPa in the two solutions, respectively, and the average value 3.67 cm^{-1}/GPa can be used, that is, $\Delta\Omega_2(P) = \Delta\Omega_1(P) = 3.67 \times P$. Therefore, the contribution of VC to the variations of adiabatic frequency can then be expressed as

$$\Delta(\mathrm{VC}) = 3.67 \times P - \Delta\omega_1 \quad (5)$$

according to eq 4, where $\Delta\omega_1$ is the total change of the adiabatic frequency. By using of the slopes of the $\nu1$ bands shown in Figures 3 (2.13 cm^{-1}/GPa) and 4 (−0.84 cm^{-1}/GPa), Δ(VC) can be calculated using eq 5 to achieve $3.67 \times 1.3 - 2.13 \times 1.3 \approx 2.0$ (cm^{-1}) and $3.67 \times 1.3 + 0.84 \times 1.3 \approx 5.9$ (cm^{-1}) in *n*-hexane and CS_2 solutions, respectively. The contribution of VC in CS_2 is about 3 times that in *n*-hexane in the considered range of pressure. This can be ascribed to the joint contribution of the increased adiabatic vibronic integral and the decreased energy gap between the S_0 and S_1 states.

B. Effect of Pressure on Spectral Bandwidth of the C═C Stretching Raman Band. We also examined the spectral bandwidth and the relative intensity of representative Raman bands. The most visible pressure dependence of spectral width is found in CS_2 solution for the $\nu1$ band. As shown in Figure 6, the bandwidth (full-width at half-maximum, fwhm) of the C═C stretching mode increases ∼13 cm^{-1} from ambient pressure to 4.6 GPa.

The effect of solvent on the bandwidth of the C═C stretching resonance Raman band in both the S_1 and S_0 states is neglectable for nonpolar β-carotene molecules.[10] The broader bandwidth of this band in S_1 relative to its width in S_0 was ascribed to the shorter vibrational relaxation time in the S_1 state.[10] When the molecule is compressed, the increased force constant leads to a

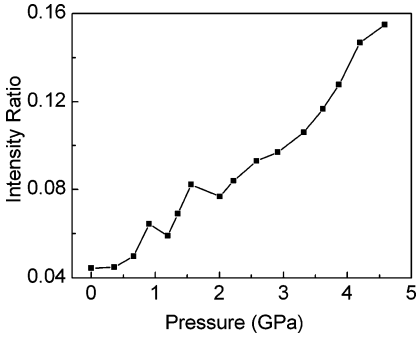

Figure 7. Intensity ratio of the $\nu 4$ to $\nu 2$ bands versus pressure in CS_2.

decreased vibrational cycle, and a faster relaxation rate is expected. Therefore, the broader bandwidth is ascribed to the shorter vibrational relaxation time under high pressure. The bandwidth at normal pressure ($\sim$20 cm^{-1}) corresponds to a relaxation time of $\sim$250 fs, while at 4.6 GPa, it ($\sim$33 cm^{-1}) corresponds to $\sim$150 fs.

It can be concluded from this result that the vibrational relaxation rate in the excited states should also be increased under high pressure. As the absorption spectra (Figure 5) have revealed the decreased energy gap between electronic states, the rate of IC and IVR will surely be accelerated by high pressure. In the case of carotenoids in the light-harvesting complexes, the lifetime becomes shorter due to the ultrafast energy-transfer reactions from carotenoids to bacteriochlorophyll.[25] The IC and IVR processes are competitive with the energy-transfer reactions from carotenoids to bacteriochlorophyll in the light-harvesting complexes; therefore, the investigation of carotenoids in solution under high pressure may present a novel insight for elucidating some ultrafast dynamics properties of carotenoids in vivo.

C. Effect of Pressure on the Relative Intensity of the $\nu 4$ and $\nu 2$ Bands. The Raman intensities of out-of-plane vibrations are associated with the distortion of the carotenoid molecular conformation from a plane.[19] Figure 7 shows the pressure dependence of the integral intensity ratio of the $\nu 4$ to $\nu 2$ bands. The enhanced intensity of the $\nu 4$ band, also shown in Figure 2, is associated with the structural distortion of β-carotene molecules. It can therefore be concluded that β-carotene molecules have undergone a structural distortion in the whole conjugated chain under high pressure, although no *cis* isomer appeared. It is well-known that the intensity of Raman spectra is determined by the gradients of the polarizability tensor with respect to normal coordinates. The visible enhancement of the $\nu 4$ band indicates a large change in polarizability for this mode. It can therefore be concluded that the large change in polarizability for the C−H out-of-plane wagging mode is rooted in the distortion of molecular structure. This conclusion is in good agreement with normal coordinate analysis.[19]

In addition, the distorted configuration shortens the effective length of the conjugated chain; a blue shift of the absorption spectrum can be expected for merely a structural consideration.[26] However, the experimental result is a red shift of the absorption spectrum under high pressure, as shown in Figure 5, which can be explained in terms of the solvent index of refraction changes. It can be therefore concluded that the environmental factor, rather than the slight structural deformation, is the primary cause of the spectral changes under high pressure. This is the reason why we ignore the contributions of structural distortion to the Raman frequency shifts in our competitive mechanism.

Another factor that affects the ground-state frequency of the C═C stretching in polyene is the degree of conjugation through the π-electron system. The decrease of the C═C stretching vibration frequency for polyene of increased chain length has been explained by assuming that, with the increase of the chain length, the π-electrons delocalization tends to equalize the CC bond lengths, thereby decreasing the bond order of C═C bonds and causing a lower C═C stretching frequency for longer polyene.[27] Weesie et al. used this assumption to explain the frequency shift of the $\nu 1$ line in the solid state and in solution.[4] Accordingly, for the distorted β-carotene molecules, which have a relatively shorter effective length of the conjugated chain, the frequency of the $\nu 1$ band shifts to a larger wavenumber. However, our experimental result obtained with β-carotene in CS_2 solution is a downward shift of the $\nu 1$ frequency in the liquid phase, and this means that the degree of conjugation through the π-electron system is not changed for the distortion of molecular configuration. This conclusion is also supported by the quantum chemical calculations made for polyenes with different chain lengths.[28]

All of these results support our opinion; besides the bond length changes, VC, rather than the structural distortion or π-electrons delocalization, is the primary reason for the Raman spectral changes under high pressure.

Conclusion

It is found through the investigation of Raman spectra of β-carotene in *n*-hexane and CS_2 solutions under quasi-hydrostatic pressure conditions that the β-carotene molecule is chemically stable and no *cis* isomer appears throughout the 0−4.6 Gpa range of pressures in our experimental conditions (room temperature, excitation wavelength of 632.8 nm). The effect of solvent polarizability on VC between the S_0 and S_1 states of β-carotene is first reviewed with the aid of high pressure. A competitive mechanism involving VC and bond length changes is used to explain the diverse pressure effect on the Raman frequency of the $\nu 1$ and $\nu 2$ bands in different solutions, and this mechanism can also lead to the prevalent viewpoint that the in-phase C═C symmetric stretching mode plays a very important role in the $S_1 \rightarrow S_0$ nonradiative internal conversion process of carotenoids. The visible broadening of the C═C stretching Raman band predicates the accelerated process of IC and IVR under high pressure. In addition, the conjugated chain of β-carotene molecules undergoes a structural distortion under high pressure, although no *cis* isomeric compound appears. The environment effect, which is related to VC but not the structural distortion or π-electrons delocalization, is responsible for the spectral properties of carotenoids at normal and high pressure. The function of a given carotenoid species in vivo is directly relevant to the ambient (protein) environments. These results indicate that high pressure, combined with spectroscopy and the effect of solvent, can provide a novel insight for elucidating the photophysical and photochemical functions of carotenoids.

Acknowledgment. We thank the National Natural Science Foundation of China (Grant Nos. 10774034, 10674034, 60478015, and 10504005) for its financial support.

References and Notes

(1) Frank, H. A.; Cogdell, R. J. *Photochem. Photobiol*. **1996**, *63*, 257.

(2) Koyama, Y.; Kuki, M.; Andersson, P. O.; Gillbro, T. *Photochem. Photobiol.* **1996**, *63*, 243.

(3) Polívka, T.; Sundström, V. *Chem. Rev.* **2004**, *104*, 2021.

(4) Weesie, R. J.; Merlin, J. C.; Lugtenburg, J.; Britton, G.; Jansen, F. J. H. M.; Cornard, J. P. *Biospectroscopy* **1999**, *5*, 19.

(5) Pendon, Z. D.; Gibson, G. N.; van der Hoef, I.; Lugtenburg, J.; Frank, H. A. *J. Phys. Chem. B* **2005**, *109*, 21172.

(6) Auerbach, R. A.; Christensen, R. L.; Granville, M. F.; Kohler, B. E. *J. Chem. Phys.* **1981**, *74*, 4.

(7) Zerbetto, F.; Zgierski, M. Z.; Orlandi, G.; Marconi, G. *J. Chem. Phys.* **1987**, *87*, 2505.

(8) Nagae, H.; Kuki, M.; Zhang, J. P.; Sashima, T.; Mukai, Y.; Koyama, Y. *J. Phys. Chem. A* **2000**, *104*, 4155.

(9) Hashimoto, H.; Koyama, Y. *Chem. Phys. Lett.* **1989**, *154*, 321.

(10) Noguchi, T.; Hayashi, H.; Tasumi, M.; Atkinson, G. H. *J. Phys. Chem.* **1991**, *95*, 3167.

(11) Wasielewski, M. R.; Johnson, D. G.; Bradford, E. G.; Kispert, L. D. *J. Chem. Phys.* **1989**, *91*, 6691.

(12) Yoshizawa, M.; Aoki, H.; Hashimoto, H. *Phys. Rev. B* **2001**, *63*, 180301.

(13) Kukura, P.; McCamant, D. W.; Mathies, R. A. *J. Phys. Chem. A* **2004**, *108*, 5921.

(14) Kuki, M.; Nagae, H.; Cogdell, R. J.; Shimada, K.; Koyama, Y. *Photochem. Photobiol.* **1994**, *59*, 116.

(15) Ho, Z. Z.; Moore, T. A.; Lin, S. H.; Hanson, R. C. *J. Chem. Phys.* **1981**, *74*, 873.

(16) Ho, Z. Z.; Hanson, R. C.; Lin, S. H. *J. Phys. Chem.* **1985**, *89*, 1019.

(17) Piermarini, G. J.; Block, S. *Rev. Sci. Instrum.* **1975**, *46*, 973.

(18) Mao, H. K.; Bell, P. M.; Shaner, J. V.; Steinberg, D. J. *J. Appl. Phys.* **1978**, *49*, 3276.

(19) Saito, S.; Tasumi, M. *J. Raman Spectrosc.* **1983**, *14*, 310.

(20) Wang, H.; Zheng, H. F.; Sun, Q. *Appl. Spectrosc.* **2005**, *59*, 1498.

(21) Ishizumi, A.; Kasami, M.; Mishina, T.; Yamamoto, S.; Nakahara, J. *High Pressure Res.* **2003**, *23*, 201.

(22) Moroni, L.; Ceppatelli, M.; Gellini, C.; Salvi, P. R.; Bini, R. *Phys. Chem. Chem. Phys.* **2002**, *4*, 5761.

(23) Hashimoto, H.; Koyama, Y. *J. Phys. Chem.* **1988**, *92*, 2101.

(24) Watanabe, Y.; Kameyama, T.; Miki, Y.; Kuki, M.; Koyama, Y. *Chem. Phys. Lett.* **1993**, *206*, 62.

(25) Zhang, J. P.; Fujii, R.; Qian, P.; Inaba, T.; Mizoguchi, T.; Koyama, Y.; Onaka, K.; Watanabe, Y.; Nagae, H. *J. Phys. Chem. B* **2000**, *104*, 3683.

(26) Andersson, P. O.; Bachilo, S. M.; Chen, R. L.; Gillbro, T. *J. Phys. Chem.* **1995**, *99*, 16199.

(27) Rimai, L.; Heyde, M. E.; Gill, D. *J. Am. Chem. Soc.* **1973**, *95*, 4493.

(28) OrLandi, G.; Zerbetto, F.; Zgierski, M. Z. *Chem. Rev.* **1991**, *91*, 867.